Crystallization in Poly(L-lactide)-*b*-poly(ϵ-caprolactone) Double Crystalline Diblock Copolymers: A Study Using X-ray Scattering, Differential Scanning Calorimetry, and Polarized Optical Microscopy

I. W. Hamley* and V. Castelletto

Centre for Self-Organizing Molecular Systems and Department of Chemistry, University of Leeds, Leeds LS2 9JT, UK

R. V. Castillo and A. J. Müller*

Grupo de Polímeros USB, Departamento de Ciencia de los Materiales, Universidad Simón Bolívar, Apartado 89000, Caracas 1080-A, Venezuela

C. M. Martin

Synchrotron Radiation Source, CLRC Daresbury Laboratory, Warrington WA4 4AD, UK

E. Pollet and Ph. Dubois

Service des Materiaux Polymères et Composites SMPC, Université de Mons-Hainaut, Place du Parc 20, B-7000 Mons, Belgium

Received September 9, 2004; Revised Manuscript Received October 27, 2004

ABSTRACT: The crystallization of well-defined poly(L-lactide)-*b*-poly(ϵ-caprolactone) diblock copolymers, PLLA-*b*-PCL, was investigated by time-resolved X-ray techniques, polarized optical microscopy (POM), and differential scanning calorimetry (DSC). Two compositions were studied that contained 44 and 60 wt % poly(L-lactide), PLLA (they are referred to as $L_{44}{}^{11}C_{56}{}^{14}$ and $L_{60}{}^{12}C_{40}{}^{9}$, respectively, with the molecular weight of each block in kg/mol as superscript). The copolymers were found to be initially miscible in the melt according to small-angle X-ray scattering measurements (SAXS). Their thermal behavior was also indicative of samples whose crystallization proceeds from a mixed melt. Sequential isothermal crystallization from the melt at 100 °C (for 30 min) and then at 30 °C (for 15 min) was measured. At 100 °C only the PLLA block is capable of crystallization, and its crystallization kinetics was followed by both WAXS and DSC; comparable results were obtained that indicated an instantaneous nucleation with three-dimensional superstructures (Avrami index of approximately 3). The spherulitic nature of the superstructure was confirmed by POM. When the temperature was decreased to 30 °C, the PCL block was able to crystallize within the PLLA negative spherulites (with an Avrami index of 2, as opposed to 3 in homo-PCL), and its crystallization rate was much slower than an equivalent homo-PCL. Time-resolved SAXS experiments in $L_{60}{}^{12}C_{40}{}^{9}$ revealed an initial melt mixed morphology at 165 °C that upon cooling transformed into a transient microphase-separated lamellar structure prior to crystallization at 100 °C.

Introduction

Self-assembly in block copolymers is usually triggered by the thermodynamic repulsion between the covalently bonded chains that provokes microphase segregation below the order−disorder transition temperature (T_{ODT}) and the generation of fascinating morphologies.[1] Crystallization usually complicates the morphological features of block copolymers since it competes with phase segregation. Depending on the segregation strength and on the relative values of the glass transition temperature (T_g), the crystallization temperature (T_c) and the T_{ODT} many different morphologies can be generated. Depending on the segregation strength in the melt, either crystallization can be confined within the copolymer microdomain structure for strongly segregated systems or crystallization can drive structure formation for weakly segregated melts (overwriting any previous microdomain structure) or homogeneous systems. Several recent reviews deal with semicrystalline block copolymer properties.[2−4]

The synthesis of biodegradable block copolymers with polyester building blocks has attracted much recent interest in view of their numerous biomedical applications.[5] However, few studies can be found that are devoted to the crystallization and structure of complex double crystalline well-defined diblock copolymers that are at the same time biodegradable.[6−13] We have previously studied the morphology, nucleation, and crystallization kinetics of poly(p-dioxanone)-*b*-poly(ϵ-caprolactone) diblock copolymers.[6−8] The combination of building blocks that are quickly degraded by hydrolysis (like poly(*p*-dioxanone) or polylactides) with the much more stable poly(ϵ-caprolactone) can yield materials with tunable lifetime for in vivo applications.

Two previous works on the crystallization of well-defined poly(L-lactide)-*b*-poly(ϵ-caprolactone) diblock copolymers, PLLA-*b*-PCL, have recently been published.[10−11] Kim et al.[10] report the synthesis and characterization of PLLA-*b*-PCL employing a macroinitiator of hydroxyl-terminated PCL followed by ring-opening polymerization of L-lactide. They obtained polymers with polydispersities in the range 1.3−1.6. For a copolymer containing 32 wt % PCL and a number-average molecular weight, M_n, of 77 000 g/mol they found by rheological measurements a T_{ODT} of 220 °C. In the case of another sample containing 37.4 wt % PCL and 19 000

* Authors for correspondence.

10.1021/ma0481499 CCC: $30.25
Published on Web 12/15/2004

g/mol they found a homogeneous melt just above the melting point of the PLLA block at 175 °C. Kim et al.[10] investigated the crystallization of the PLLA block only, since they employed high crystallization temperatures (T_c) at which the PCL block was molten.

The segregation strength is usually expressed[1] for block copolymers as the product of the Flory−Huggins interaction parameter and the block copolymer degree of polymerization: χN. In the particular case of PLLA-*b*-PCL, Ho et al.[11] have roughly estimated χN to be in the range 2.9−4 for a temperature range from 180 to 50 °C for a polymer with an M_n value of 23 600 g/mol and a 73.7 wt % PLLA content. Since these values are quite low in comparison with the expectation of the mean-field theory for block copolymers in the weak segregation regime, it is expected that the crystallization proceeds from a mixed melt. Furthermore, the morphology obtained was consistent with crystallization from a melt mixed system.[11] In this investigation, Ho et al. demonstrated the feasibility of preparing large sized well-oriented microdomains of PLLA-*b*-PCL employing different crystalline substrates like benzoic acid and hexamethylbenzene.

In this work, we investigate the structure and crystallization of both the PLLA and the PCL blocks within PLLA-*b*-PCL diblock copolymers employing time-resolved SAXS (small-angle X-ray scattering) and WAXS (wide-angle X-ray scattering) techniques as well as DSC (differential scanning calorimetry) and POM (polarized optical microscopy).

Experimental Section

Synthesis. PLLA-*b*-PCL diblock copolymers were synthesized by controlled/"living" sequential block copolymerization as initiated by aluminum trialkoxides in toluene solution.[14]

Materials. ϵ-Caprolactone (CL) from Acros was dried over CaH_2 for 48 h, distilled under reduced pressure, and stored under inert atmosphere. LL-Dilactide (LA) (≥99%, from Boehringer, Ingelheim, Germany), crystallized from toluene, was purified just before use by sublimation under vacuum (10^{-3} mbar, 85 °C). Aluminum triisopropoxide ($Al(O^iPr)_3$) from Acros was distilled under reduced pressure in a previously flamed and nitrogen-purged conventional apparatus. Condensed at the temperature of liquid nitrogen, $Al(O^iPr)_3$ was allowed to warm to room temperature, rapidly dissolved in dry toluene, and stored under a nitrogen atmosphere. The accurate solution concentration was determined by back complexometric aqueous titration of Al^{3+} with standard solutions of Na_2EDTA and $ZnSO_4$ at pH 4.8. 2-Propanol from Aldrich was dried with calcium hydride and distilled under vacuum. Toluene (99%, from Labscan) was dried by refluxing over calcium hydride for at least 48 h and distilled under a N_2 atmosphere just before use.

Instrumentation. ^{1}H NMR spectra were recorded using a Bruker AMX300 spectrometer at room temperature in $CDCl_3$ (10 mg/0.6 mL). Size exclusion chromatography (SEC) was performed in THF at 35 °C using a Polymer Laboratories liquid chromatograph equipped with a PL-DG802 degasser, an isocratic HPLC pump LC 1120 (1 mL/min flow rate), a Marathon autosampler (200 μL loop volume, 1 mg/mL solution concentration), a PL-DRI refractive index detector, and a set of three columns: a PL gel 10 μm guard column and two PL gel Mixed-B 10 μm columns. Molar masses and molar masses distribution were calculated with reference to polystyrene standards. Molecular weights and molecular weight distribution were calculated with reference to polystyrene standards. The absolute average-number molecular weight (M_n) of PCL was calculated using a universal calibration curve and polystyrene standards in THF at 35 °C (K for PS = 1.25×10^{-4} dL/g, a for PS = 0.707; K for PCL = 1.09×10^{-3} dL/g, a for PCL = 0.600 in the $[\eta] = KM^a$ or Khun−Mark−Houwink relationship). Molecular weight and molecular weight distribution for PLLA homopolymer were calculated by reference to a universal calibration curve relative to PS standard and using the Kuhn−Mark−Houwink equation for PLLA in THF: $M_n(PLA) = 0.4055 \times M_n(PS)1.0486$.

Table 1. Molecular Characteristics of the Block Copolymers and Homopolymers

sample code	PLLA/PCL exp comp[a]	$M_{n,exp}$[b] PLLA block	$M_{n,exp}$[c] PCL block	I[d]
$PLLA^{24}$	100/0	23 900		1.1
$L_{60}{}^{12}C_{40}{}^{9}$	60/40	12 400	8 500	1.1
$L_{44}{}^{11}C_{56}{}^{14}$	44/56	11 100	14 200	1.3
PCL^{29}	0/100		28 900	1.3

[a] Experimental composition as determined by ^{1}H NMR. [b] Calculated M_n estimated by ^{1}H NMR for the PLLA block knowing the M_n of the PCL block determined by SEC. [c] Experimental M_n estimated by SEC for the PCL block. [d] Polydispersity index of the final copolymer (determined by SEC).

Procedure. First, ϵ-CL polymerization was initiated by $Al(OiPr)_3$ in toluene solution at 25 °C for 48 h. Then, LL-lactide was added and polymerized at 70 °C for 7 days. Because of the reactivity difference of $Al(O^iPr)_3$ toward the two monomers (ca. 1 active alkoxide site per Al atom for ϵ-CL vs 3 active sites per Al atom for LA), 3 equiv of dried 2-propanol was added to the starting polymerization medium in order to activate all aluminum alkoxide groups and to avoid formation of PLLA homopolymer during the second step. After polymerization and hydrolytic deactivation of the active aluminum alkoxide species by adding some drops of diluted HCl, the (co)polyesters were isolated by selective precipitation from an excess of cold methanol. Catalyst residues were removed out before characterization as reported by Dubois et al.[14] Part of the reaction medium was picked out before adding lactide in order to determine the PCL block parameters by ^{1}H NMR and SEC (see Table 1). For the sake of comparison, two homopolyesters, PCL and PLLA, have been synthesized as well.

Physical Characterization. *SAXS/WAXS.* Simultaneous small-angle and wide-angle X-ray scattering experiments were performed on station 6.2 at the Synchrotron Radiation Source, Daresbury Lab, UK.[15,16] Samples contained in DSC pans modified to incorporate mica windows to allow transmission of the X-ray beam were mounted in a Linkam DSC cell of single pan design for thermal treatment. The X-ray wavelength was $\lambda = 1.40$ Å. Simultaneous SAXS and WAXS data were collected on a pair of one-dimensional micro-gap wire detectors based on the RAPID2 system.[15] The SAXS detector had a quadrant design, and the WAXS detector was curved with a 60° 2θ acceptance angle. The wavenumber $q = 4\pi \sin \theta/\lambda$ for SAXS was calibrated using rat-tail collagen, and the WAXS angular scale was calibrated using NBS silicon and high-density polyethylene.

DSC. A Perkin-Elmer DSC-7 power compensated differential scanning calorimeter was employed. Samples with approximately 5 mg in weight were encapsulated in aluminum pans. The equipment was calibrated with indium and hexatriacontane, and an ultrapure nitrogen atmosphere was employed as circulating atmosphere. Measurements during cooling and heating at 10 °C/min as well as in isothermal mode were performed.

POM. The superstructural morphology was observed in thin films prepared between microscope coverslips by melting the polymer at 190 °C for 3 min and then quickly cooling to the isothermal crystallization temperature in a Linkam TP-91 hot stage. The samples were placed between crossed polarizers in a Zeiss MC-80 optical microscope equipped with a camera system. To enhance contrast and determine the sign of the spherulites, a λ wave plate was inserted between the polarizers.

All samples for SAXS/WAXS, DSC, and POM were prepared by solvent evaporation from chloroform solutions.

Results and Discussion

Figure 1 shows DSC cooling scans (performed at 10 °C/min) of the two diblock copolymers and equivalent

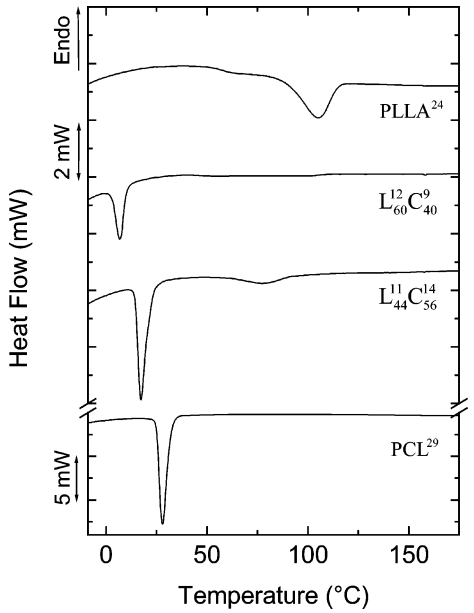

Figure 1. DSC cooling scans at 10 °C/min, after melting at 200 °C for 3 min.

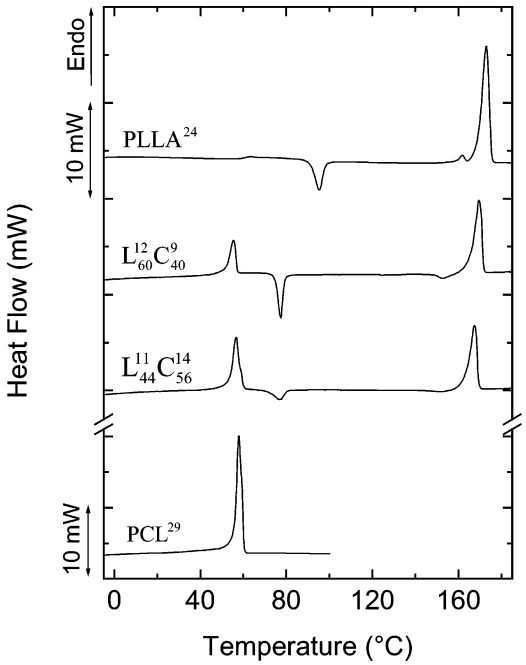

Figure 2. DSC subsequent heating scans (at 10 °C/min) to the cooling scans presented in Figure 1.

homopolymers and Figure 2 shows subsequent heating scans while Table 2 lists the observable transition enthalpies and temperatures. Previous estimates of χN values for the PLLA-*b*-PCL diblock copolymers indicate that they are well below 10 for the temperatures and molecular weight ranges employed here, so miscibility in the melt is expected and has been previously observed.[11] The results presented in Figures 1 and 2 and in Table 2 also indicate that the system is miscible in the melt and undergoes phase segregation when each block crystallizes. Our SAXS experiments performed in the melt also support the initial miscibility of the diblock copolymers at temperatures ranging from 190 to 160 °C (see below).

Figure 1 shows that the PLLA block within $L_{60}{}^{12}C_{40}{}^{9}$ crystallizes during cooling from the melt at lower temperatures than PLLA homopolymer and to a much lower extent. This is a consequence of the miscibility of the system. The T_g of PLLA can be clearly observed in the heating scan of Figure 2 at 59.8 °C. The corresponding T_g for PCL is at −63 °C (results not shown). In the block copolymers, the T_g of the semicrystalline blocks is difficult to detect by DSC. Using the Fox equation[17] to determine an approximate value of the T_g of a miscible system, a T_g value of approximately −1 °C can be obtained for $L_{60}{}^{12}C_{40}{}^{9}$. The T_g of the system decreases to −20 °C, according to the Fox equation, for the copolymer with a higher amount of PCL (i.e., $L_{44}{}^{11}C_{56}{}^{14}$); this is the reason why the PLLA block within $L_{44}{}^{11}C_{56}{}^{14}$ crystallizes more than $L_{60}{}^{12}C_{40}{}^{9}$, and its crystallization temperature is shifted to lower values (see Table 2).

The PCL block in the copolymers also crystallizes during cooling from the melt and at lower temperatures when compared to that of the PCL homopolymer. For the $L_{44}{}^{11}C_{56}{}^{14}$diblock copolymer the crystallization of the PCL block occurs at lower temperatures and to a much lower extent than for $L_{60}{}^{12}C_{40}{}^{9}$, a fact that may also be related to the relative T_g values of the amorphous phase. The heating runs presented in Figure 2 reflect the expected behavior after the cooling scans in Figure 1. The peak melting point of the PLLA block in the copolymers is lower than in the homopolymer and decreases as the content of PCL increases, a fact that is consistent with a mixed amorphous phase. Invariance of T_m with block copolymer composition would be expected for immiscible polymer pairs in the composition range studied here.[1−4] The cold crystallization of PLLA is more pronounced in $L_{60}{}^{12}C_{40}{}^{9}$, the copolymer where the crystallization during the cooling scan was more hindered. The PCL block also shows a slight depression of its T_m value which is probably related to the previous crystallization behavior.

That both PCL and PLLA blocks were crystalline at room temperature was confirmed by WAXS. Figure 3 compares a typical WAXS pattern for $L_{44}{}^{11}C_{56}{}^{14}$ with data for each homopolymer in the crystalline state. The very strong peak at $2\theta = 14.8°$ corresponds closely to the $110/1\bar{1}0/200$ reflections at $2\theta = 15.083°$ and 15.093° of the α-form of PLLA. (The powder diffraction pattern was calculated using the crystallographic information in ref 18.) The next peak at $2\theta = 17.0°$ is close to the position expected for the sets of 113 and 203 reflections of the α-form of PLLA, $2\theta = 17.259°$ and $2\theta = 17.268°$.[18]

Table 2. Thermal Properties Obtained from DSC Scans Presented in Figures 1 and 2

	PCL					PLLA					
sample	T_c (°C)	T_m (°C)	ΔH_c (J/g)	ΔH_m (J/g)	T_g (°C)	$T_c{}^a$ (°C)	$T_c{}^b$ (°C)	T_m (°C)	$\Delta H_c{}^a$ (J/g)	$\Delta H_c{}^b$ (J/g)	ΔH_m (J/g)
$PLLA^{24}$					59.8	105.0	95.2	173.0	29	17	68
$L_{60}{}^{12}C_{40}{}^{9}$	6.8	55.4	27	41		97.8	77.4−152.9	169.5	−6	27−7	69
$L_{44}{}^{11}C_{56}{}^{14}$	17.3	56.5	40	49		78	76.9−151.4	167.5	12	17−2	75
PCL^{29}	28.0	58.0	63	68							

[a] Values of crystallization temperatures and enthalpies of PLLA during cooling scans. [b] Values of crystallization temperatures and enthalpies of PLLA during heating scans.

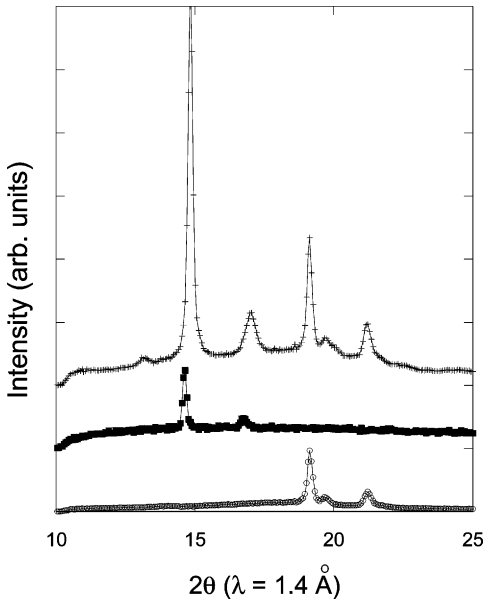

Figure 3. WAXS data: (+) block copolymer $L_{44}{}^{11}C_{56}{}^{14}$, (■) PLLA homopolymer, (○) PCL homopolymer. Data for block copolymer and PCL homopolymer recorded at 30 °C, and data for PLLA recorded at 100 °C. The lines are guides to the eye.

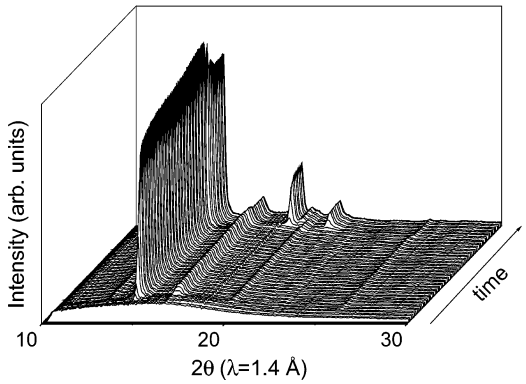

Figure 4. WAXS data for block copolymer $L_{44}{}^{11}C_{56}{}^{14}$ obtained starting at 190 °C, quenching at 50 °C/min to 100 °C where PLLA crystallizes (30 min hold), and then quenching at 50 °C/min to 30 °C (15 min hold) where PCL crystallizes.

It is noticeable that the two PLLA peaks from the PLLA block in $L_{44}{}^{11}C_{56}{}^{14}$ are shifted significantly to higher angle as compared to those for the homopolymer, pointing to a reduction in unit cell parameters. A similar effect was observed for $L_{60}{}^{12}C_{40}{}^{9}$, although to a lesser extent. This is not the case for the PCL block. Three strong peaks at larger 2θ are in the same position as those for PCL homopolymer. The first reflection at $2\theta = 19.2°$ is close to the position of the 110 reflection of PCL, and the shoulder at $2\theta = 19.8°$ may be the 111 peak, although its position is shifted from that expected ($2\theta = 20.02°$) based on the published crystal structure.[19] The final prominent peak is the 200 peak from PCL.

The crystallization of PCL and PLLA in the block copolymers was confirmed by step cooling experiments, starting from the melt at a temperature $T = 190$ °C above the melting point of both blocks. The first quench was to $T = 100$ °C, at which temperature PLLA crystallizes (peak $T_c = 95$ °C for PLLA homopolymer from DSC, see Table 2), and then to 30 °C, where PCL crystallizes also (the temperature profile is shown in Figure 6).

Figure 4 shows time-resolved WAXS data obtained during the sequence of experiments described above for

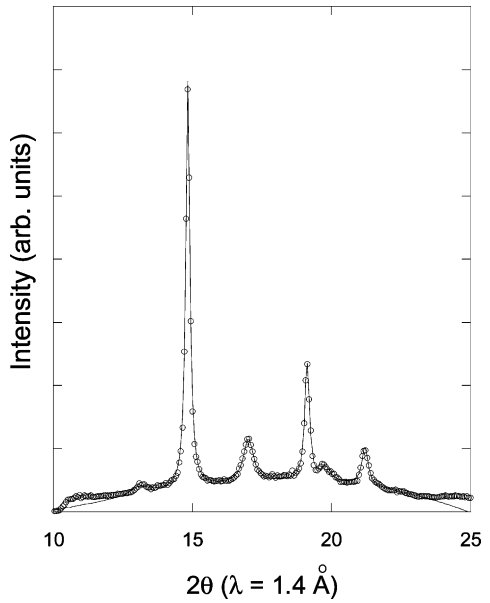

Figure 5. (○) WAXS data for block copolymer $L_{44}{}^{11}C_{56}{}^{14}$ at 30 °C, when both blocks have crystallized. The solid line indicates a fit to six Lorentzian functions with a cubic polynomial background.

$L_{44}{}^{11}C_{56}{}^{14}$. The rapid development of peaks from crystalline PLLA soon after the temperature reached 100 °C is evident (see also Figure 6). After 30 min at 100 °C the temperature was decreased to 30 °C. Then the appearance of the three peaks from crystalline PCL (as discussed above) is clearly seen. These grow shortly after the temperature reaches 30 °C. The peak at $2\theta = 17.7°$ that persists for the whole experiment (also in Figure 11) is due to the mica windows in the DSC pan employed for X-ray measurements.

To analyze the crystallization kinetics, the WAXS crystal peaks were fitted to a series of Lorentzian functions, with a cubic polynomial background to allow for the contribution of amorphous scattering (the background was fixed during the fitting). Figure 5 shows a representative fit for one of the final frames in Figure 4 corresponding to $L_{44}{}^{11}C_{56}{}^{14}$, where both blocks are semicrystalline. The quality of fit is excellent, allowing accurate determination of peak positions, widths, and intensities.

Figure 6 shows the evolution of peak intensities for $L_{44}{}^{11}C_{56}{}^{14}$ determined in the way previously described. The increase in intensity of the strong PLLA reflection (at $2\theta = 14.8°$) during the isothermal crystallization at 100 °C follows a sharp increasing function during the first 5 min corresponding to PLLA crystallization. Later, a slower growth of the peak intensity can be seen until the programmed 30 min at 100 °C is over; this continuous increase in intensity may correspond to the final stages of the secondary crystallization. Then a curious phenomenon occurs when the temperature was dropped to 30 °C. A sharp reduction in the peak intensity of the crystalline PLLA reflection can be seen as PCL crystallizes. The crystallization of PCL was followed by monitoring the increase in intensity of the 110 reflection of the PCL (at $2\theta = 19.2°$). This suggests a reduction in crystallinity of PLLA as PCL crystallizes. It is possible that to accommodate the crystallization of PCL some rearrangement of the PLLA chains is necessary, which is accomplished by local melting. A small increase in peak position from $2\theta = 14.71°$ to $2\theta = 14.83°$ occurs simultaneously, pointing to a change in the a and b

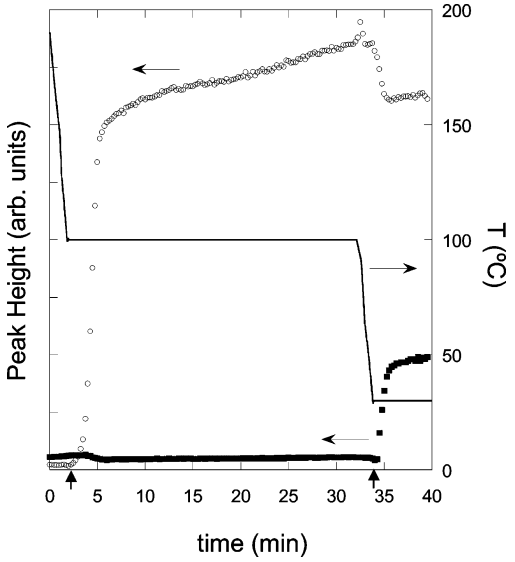

Figure 6. Height of WAXS peaks for block copolymer $L_{44}{}^{11}C_{56}{}^{14}$ from fitted Lorentzian functions: (○) $2\theta = 14.8°$ reflection of PLLA, (■) 110 reflection of PCL. The solid line indicates the temperature measured by the DSC instrument (Linkam) employed in the X-ray setup. The vertical arrows at the axis indicate the times at which the target crystallization temperature was achieved and therefore the initial time considered for fitting the Avrami equation (see Figure 9 and its discussion).

dimensions of the PLLA unit cell (i.e., a lateral contraction) in the block copolymer. Another possibility that may explain the above results is that a change in the structure factor (F_{hkl}) could occur since the unit cell is being distorted. However, SAXS evidence below (see Figure 15 and its discussion) also points to a reduction of crystallinity. It may be that both effects are taking place simultaneously.

We have reproduced by parallel DSC tests the experiments performed by WAXS in Figure 6. Figure 7 shows the isothermal crystallization exotherms obtained first at 100 °C and then at 30 °C. A cooling rate of 50 °C/min, which is identical to that employed in the WAXS experiments, was used before each isothermal crystallization period. Also included in Figure 7 is a final heating scan (at 10 °C/min) from 30 °C and where the melting endotherms of both blocks are clearly seen. Figure 8 plots the data in enthalpy as a function of time to parallel Figure 6. The behavior is analogous except that in the DSC more data points were collected during the isothermal steps.

Figure 9 compares the results obtained by DSC and WAXS. The results have been normalized by the maximum values of the variables being measured after a certain crystallization time. In this way, α_c represents the relative fraction of material that has been transformed to the crystalline state at any given time. The crystallization isotherms at 100 °C presented in Figure 9a for the PLLA block within $L_{44}{}^{11}C_{56}{}^{14}$ are in good agreement despite the intrinsic differences in the techniques employed. In the case of the PCL block the agreement is not good, partly because the X-ray data are scarce especially at the start of the crystallization.

Similar X-ray and DSC experiments were performed for the other block copolymer, i.e., $L_{60}{}^{12}C_{40}{}^{9}$. The temperature profile and fitted peak heights are shown in Figure 10, while the original frames of WAXS data are presented in Figure 11. Note that the cooling rate in the second step from 100 to 30 °C was not rapid due to

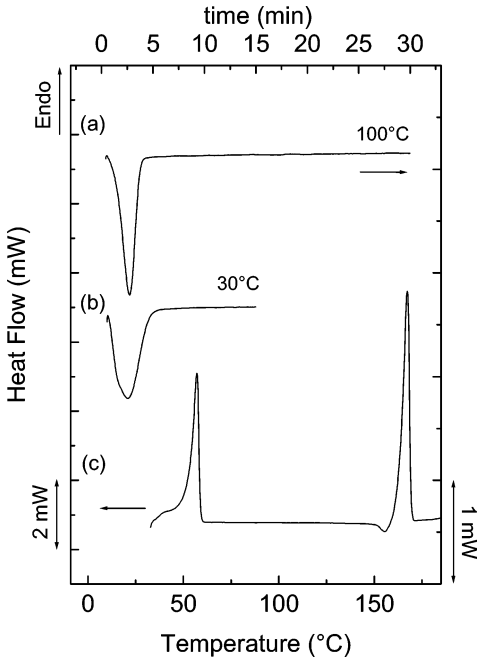

Figure 7. (a) DSC isothermal crystallization data taken at 100 °C for 30 min (a temperature at which only the PLLA block crystallizes), after cooling at 50 °C/min from 190 °C for $L_{44}{}^{11}C_{56}{}^{14}$. (b) Subsequent isothermal crystallization at 30 °C for 15 min (a temperature at which the PCL block crystallizes), after cooling at 50 °C/min from 100 °C. (c) Final subsequent DSC heating scan at 10 °C/min.

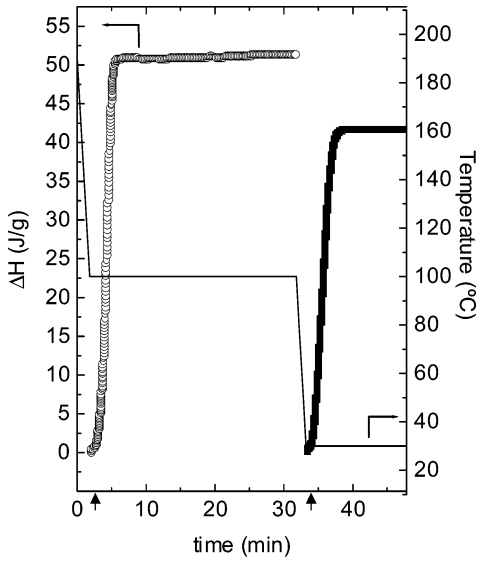

Figure 8. Crystallization enthalpies vs time (obtained from the data reported in Figure 7) for block copolymer $L_{44}{}^{11}C_{56}{}^{14}$: (○) PLLA block, (■) PCL block. The solid line indicates the temperature measured by the DSC instrument (Perkin-Elmer DSC-7). The vertical arrows at the axis indicate the times at which the target crystallization temperature was achieved and therefore the initial time considered for fitting the Avrami equation (see Figure 9 and its discussion).

a problem with the liquid nitrogen cooler. Nonetheless, these data clearly show again two independent crystallization events for the PLLA and the PCL blocks. The decrease in intensity of the $2\theta = 14.8°$ peak after the main PLLA crystallization (at times greater than 7.5 min) may be due to sample movement within the DSC pans employed for the measurements. Nevertheless, there is also again a reduction in intensity of the primary PLLA Bragg reflection (and a small shift to

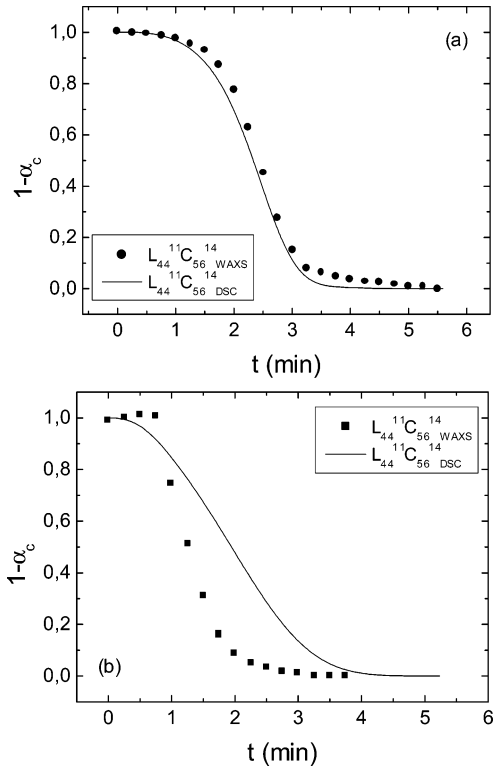

Figure 9. Plots of relative conversion vs time derived from WAXS data (data points) and DSC data (solid lines) for (a) PLLA block within $L_{44}{}^{11}C_{56}{}^{14}$ copolymer at T_c = 100 °C. (b) PCL block within $L_{44}{}^{11}C_{56}{}^{14}$ copolymer at T_c = 30 °C.

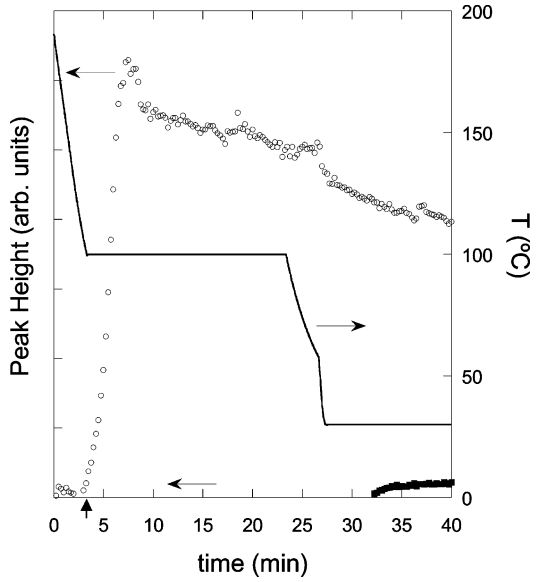

Figure 10. Height of WAXS peaks for block copolymer $L_{60}{}^{12}C_{40}{}^{9}$ from fitted Lorentzian functions: (○) 2θ = 14.8° reflection of PLLA, (■) 111 reflection of PCL. The solid line indicates the temperature measured by the DSC instrument (Linkam) employed in the X-ray setup. The vertical arrow at the axis indicate the time at which the target crystallization temperature was achieved for the PLLA block and therefore the initial time considered for fitting the Avrami equation (see Figure 13 and its discussion).

higher angle) as PCL crystallizes. Incidentally, the PCL block cannot complete its crystallization during the programmed 15 min isotherm at 30 °C. This can be clearly observed in the DSC experiment that parallels WAXS in Figure 12. Once more a good agreement between WAXS and DSC isothermal crystallization

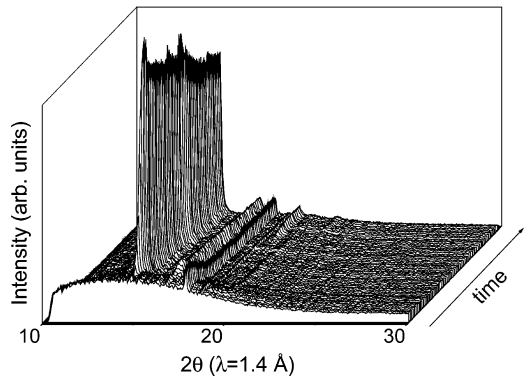

Figure 11. WAXS data for block copolymer $L_{60}{}^{12}C_{40}{}^{9}$ obtained during the temperature ramp shown in Figure 10.

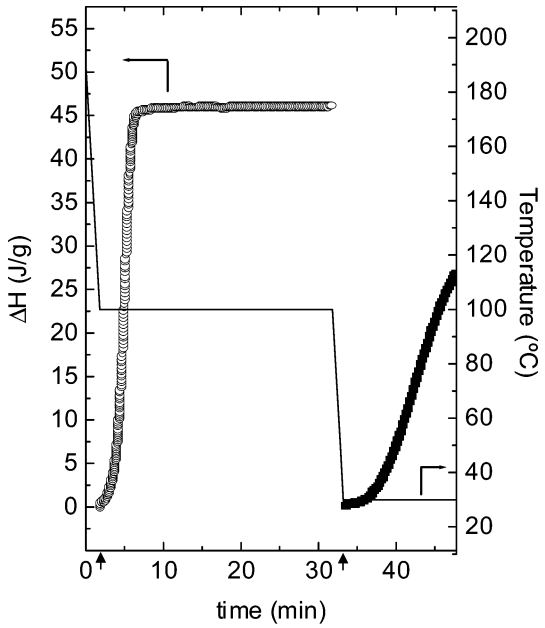

Figure 12. Crystallization enthalpies vs time for the $L_{60}{}^{12}C_{40}{}^{9}$ block copolymer: (○) PLLA block, (■) PCL block. The solid line indicates the temperature measured by the DSC instrument (Perkin-Elmer DSC-7). The vertical arrows at the axis indicate the times at which the target crystallization temperature was achieved and therefore the initial time considered for fitting the Avrami equation (see Table 3).

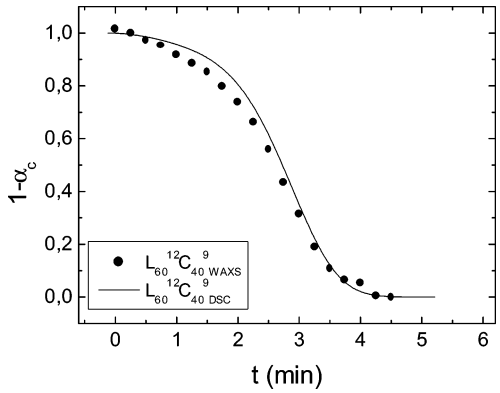

Figure 13. Plots of relative conversion vs time derived from WAXS data (data points) and DSC data (solid lines) for (a) PLLA block within $L_{60}{}^{12}C_{40}{}^{9}$ copolymer at T_c = 100 °C.

kinetic measurements can be observed for the PLLA block within $L_{60}{}^{12}C_{40}{}^{9}$ in Figure 13.

SAXS data for $L_{60}{}^{12}C_{40}{}^{9}$ obtained concurrently with the WAXS data are shown in Figure 14. Four selected

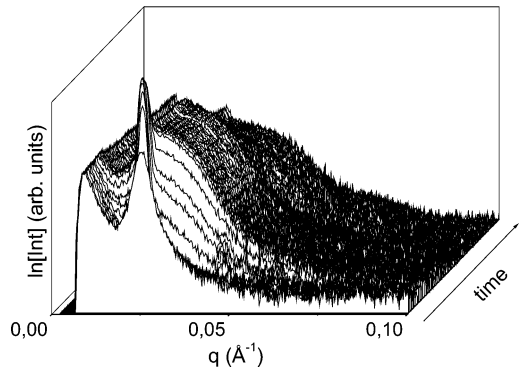

Figure 14. SAXS data for block copolymer $L_{60}{}^{12}C_{40}{}^{9}$ obtained concurrently with the WAXS data shown in Figure 11.

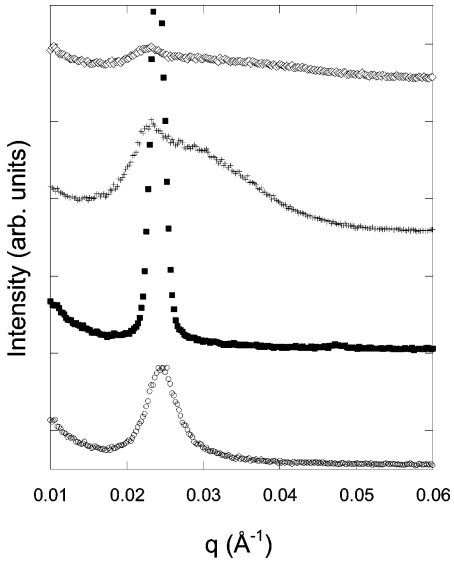

Figure 15. Selected frames of SAXS data for block copolymer $L_{60}{}^{12}C_{40}{}^{9}$ (cf. Figure 14, although here the data are shown on a linear scale): (○) in the melt on cooling from 190 °C (at approximately165 °C), (■) in the melt on cooling from 190 °C (just after reaching 100 °C), (+) at 100 °C, (◇) at 30 °C.

frames of the data presented in Figure 14 are plotted separately and are therefore better appreciated in Figure 15. The first SAXS pattern (from the bottom up) shown in Figure 15 was taken during cooling from 190 °C just as the temperature reached 165 °C, and since it shows a single sharp reflection this indicates a homogeneous melt state. It has been demonstrated previously that diblock copolymers that are being examined by SAXS at temperatures where their morphology is a homogeneous melt, produce a characteristic peak in the scattering pattern due to the correlation hole effect.[20−22] The sample was cooled further, and just when the temperature reached 100 °C the second SAXS trace shown in Figure 15 was obtained. This trace evidences a transient microphase-separated lamellar structure in the melt, since there was a strong increase in peak intensity and a higher-order reflection at $2q^*$ developed, prior to PLLA crystallization. The sharpness of the initial reflection from the melt indicates that PLLA crystallization will occur from an ordered melt. The origin of such a transient lamellar phase and whether it may be considered a precursor for the crystallization of the PLLA block are at the moment unknown; however, we expect to conduct future time-resolved X-ray experiments to investigate this phenomenon in detail.

Upon crystallization of the PLLA block within $L_{60}{}^{12}C_{40}{}^{9}$, after waiting some time at 100 °C, a sharp peak on top of a broad diffuse maximum is observed (see the third SAXS trace from the bottom up in Figure 15). The peak position shifts from $q^* = 0.0240 \pm 0.0002$ Å^{-1} (d = 262 Å) in the melt at 165 °C to $q^* = 0.0230 \pm 0.0002$ Å^{-1} (d = 273 Å) at 100 °C, where PLLA is crystalline (and a similar value at 30 °C when PCL crystallizes). The reduction in q^* is consistent with a crystalline lamellar structure with a larger domain spacing, as expected as the PLLA chains adopt a more extended conformation. Estimates of chain length within the respective crystals indicate that both blocks must be multiply folded to accommodate the chains within the measured spacings. The broad scattering feature is due to amorphous polymer.[2,20] The SAXS profile remains qualitatively similar when the crystallization of PCL occurs, although there is a reduction in peak intensity and a shift in the amorphous halo toward higher q^*, pointing to a decrease in thickness of PCL amorphous layers that accompanies the reduction in PLLA crystallinity noted above.

The isothermal crystallization data obtained by DSC and WAXS was fitted to the Avrami equation[17]

$$\alpha_c(t) = 1 - \exp(-Kt^n)$$

where $\alpha_c(t)$ is the relative crystalline volume fraction of the polymer as a function of time. The parameters K and n are dependent on the nucleation type and the crystal growth geometry, K can be considered an overall transformation rate constant, and n is the Avrami index. Typical n values for polymer spherulitic crystallization are 3 and 4. An n value of 3 indicates three-dimensional spherulitic growth from instantaneous nuclei (so-called athermal nucleation), and a value of 4 is interpreted as 3-D spherulites growing from sporadic nuclei (or thermal nucleation). If the crystallization occurs in two-dimensional aggregates (like axialites or 2-D lamellar aggregates), then Avrami indexes of 2 and 3 are expected depending on whether the nucleation is instantaneous or sporadic.[17]

Table 3 contains the results of the fit to the Avrami equation and the experimentally determined half-crystallization time ($\tau_{50\%}$); this is the time needed for a particular sample to achieve 50% of the total crystallinity the material is capable of developing during the isothermal crystallization process. The results obtained by DSC are considered first. In the case of the PLLA block, the value of $\tau_{50\%}$ is slightly lower in the diblock with 44% PLLA than in the diblock with 60%. This is probably related to their differences in T_g. The values of n are close to 3, indicating instantaneous spherulitic growth. The fact that spherulites can be form by the PLLA block at 100 °C (within the diblock copolymers) when the PCL block is molten was corroborated by POM experiments; see below (Figure 16). The values reported for homo-PLLA have been listed for comparison purposes, but according to careful DSC measurements, the material had crystallized (judging by the development of the crystallization exotherm with time, the amount it had crystallized was very small and less than 5% conversion was achieved, $\alpha_c < 0.05$) during cooling at 50 °C/min before the isothermal measurements were started; therefore, they have an implicit error which was not quantitatively determined. Nevertheless, the fact that homo-PLLA was able to crystallize during the previous cooling from the melt (even if it was a very small amount) is consistent with the cooling scans

Table 3. Avrami Parameters Obtained by Fitting Isothermal Crystallization Data Obtained by DSC and WAXS

	PCL (T_c = 30 °C				PLLA (T_c = 100 °C) DSC				PLLA (T_c = 100 °C) WAXS			
sample	n	K (min^{-n})	$\tau_{50\%}$ (min)	R^2	n	K (min^{-n})	$\tau_{50\%}$ (min)	R^2	n	K (min^{-n})	$\tau_{50\%}$ (min)	R^2
PLLA[24]					2.27[c]	0.0972[c]	2.48[c]	0.9999[c]				
$L_{60}{}^{12}C_{40}{}^{9}$	2.39[a]	0.0035[a]	9.15[a]	0.9999[a]	3.01	0.0220	2.88	0.9961	2.77	0.0414	2.67	0.9966
$L_{44}{}^{11}C_{56}{}^{14}$	2.20	0.1598[b]	1.98[b]	0.9997[b]	3.13	0.0554	2.13	0.9992	4.98	0.0080	2.42	0.9990
PCL[29]	2.95	7.7182	0.43	0.9971								

[a] The PCL block in this copolymer was crystallized until saturation for 30 min after the previous crystallization of the PLLA block (see text). [b] The PCL block in this copolymer was crystallized until saturation for 15 min after the previous crystallization of the PLLA block (see text). [c] In this sample a small amount of crystallization occurred during the quenching from the melt to T_c (see text).

shown in Figure 1 where homo-PLLA exhibited the highest peak crystallization temperature.

In the case of the PCL block, it should be remembered that the PLLA block was previously crystallized for 30 min at 100 °C, and then the sample was quenched to 30 °C and left to crystallize for 15 min. This previous crystallization of PLLA causes a dramatic difference in the crystallization kinetics of the PCL block, in view of the topological restrictions encountered by chains covalently linked to a previously crystallized PLLA block that has already arranged its crystalline lamellae into three-dimensional superstructures, leaving only lamellar slots available for PCL crystallization (i.e., the interlamellar amorphous regions). The crystallization time of 15 min was enough for homo-PCL to crystallize until saturation (i.e., $\alpha_c = 1$). For the PCL block within $L_{44}{}^{11}C_{56}{}^{14}$, the crystallization was also completed in the 15 min interval, but the kinetics was substantially slower, as can be seen from the 4-fold increase in $\tau_{50\%}$ as compared with homo-PCL. When the PLLA content increases in the copolymer, i.e., $L_{60}{}^{12}C_{40}{}^{9}$, the PCL block crystallization slows down so much that 15 min is not enough for the crystallization process to be completed, as indicated in Figure 12. Nevertheless, we repeated the DSC experiment for a longer time to allow full conversion, and the values are reported in Table 3 for $L_{60}{}^{12}C_{40}{}^{9}$. In this way, we can compare $\tau_{50\%}$ thus obtained, and as anticipated the value for $L_{60}{}^{12}C_{40}{}^{9}$ is the highest from the three values reported in Table 3 for PCL or PCL blocks; it amounts to 21 times higher than the value corresponding to homo-PCL. When the PLLA content increases, the topological restrictions must therefore also increase. Apart from this, the T_g value also goes up as PLLA content increases.

Another interesting result is that the Avrami index for the PCL block in the copolymers decreased to a value closer to 2 as compared to homo-PCL, for which the value was very close to 3 (see Table 3). This result is fully consistent with POM observations presented below, since for homo-PCL almost instantaneous spherulites are formed during crystallization at 30 °C (results not shown). However, for the PCL block within the copolymers, PLLA spherulites were previously formed (while the PCL was molten at 100 °C) and the PCL block has to crystallize within the amorphous lamellar spaces within the PLLA spherulites (see Figure 16); therefore, the dimensionality of growth is decreased to two dimensions, i.e., instantaneously nucleated lamellae.

The crystallization kinetics data obtained by WAXS were only fitted to the Avrami equation for the PLLA block of the two diblock copolymers. The PCL block crystallization was faster, and fewer data points were collected; therefore, the error in the fitting was too large (as can be seen in Figure 9b), and it is not reported in Table 3. In the case of the PLLA block the n and K values obtained are not completely satisfactory since not as many data points were collected as in the case of DSC measurements (this is reflected in lower correlation coefficients); nevertheless, they are roughly consistent with the DSC data as anticipated from the comparison presented in Figure 9a and in Figure 13.

Finally, POM results are presented in Figure 16. Parts a and b of Figure 16 present the spherulitic morphology of homo-PLLA isothermally crystallized at 100 and 120 °C, respectively. The spherulites are clearly negative in view of the characteristic colors of the Maltese cross when using a sensitive red tint plate (λ plate or first-order red gypsum plate). Quadrants 1 and 3 are close to yellow (falling colors) while 2 and 4 are blue (rising colors), a characteristic of negative spherulites.[23] This means that the highest refractive index is tangential and coincides with the chain direction. The higher nucleation density at 100 °C as compared to 120 °C is evident, and it is the expected trend with crystallization temperature.

In the case of $L_{44}{}^{11}C_{56}{}^{14}$, the sample forms PLLA spherulites at 100 °C, a temperature at which the PCL is molten (Figure 16c). This is a consistent with a mixed melt since crystallization is clearly driving structure formation when only 44% of the diblock copolymer is composed of PLLA and spherulites that are very similar to those of homo-PLLA are formed. When the sample is quenched to 30 °C and left to isothermally crystallize at that temperature, the PCL crystallization occurs within the previously formed PLLA spherulites. Figure 16d shows a micrograph taken at 30 °C after the PCL had finished crystallizing. The now mixed spherulites of the diblock copolymer are still negative, and only the magnitude of the birefringence has changed as indicated by very subtle color changes (quadrants 1 and 3 are more yellow and quadrants 3 and 4 lighter blue). Since the changes experienced by the superstructure when the PCL block crystallizes are difficult to appreciate in Figure 16c,d, the experiment was repeated at a higher temperature where larger spherulites can be obtained.

Figure 16e shows the resulting superstructure of isothermally crystallized $L_{44}{}^{11}C_{56}{}^{14}$ at 120 °C, where very clear large negative PLLA block spherulites are observed (the PCL block is molten at this temperature). Quadrants 1 and 3 are nearly red while quadrants 3 and 4 are deep blue. The spherulite is composed of PLLA crystalline lamellae that have grown radially with the chain axis located tangentially; the interlamellar regions are composed of a mixture of PLLA and PCL chains in the amorphous (liquid) state. Figure 16f–h is a sequence of micrographs taken as the PCL is isothermally crystallizing at 30 °C at increasing times. As the PCL crystallizes within the interlamellar regions of the previously formed PLLA spherulites, subtle changes in appearance and color of the spherulites can be appreciated; some yellow and blue radial lines that are particularly visible at the spherulite centers in Figure 16f

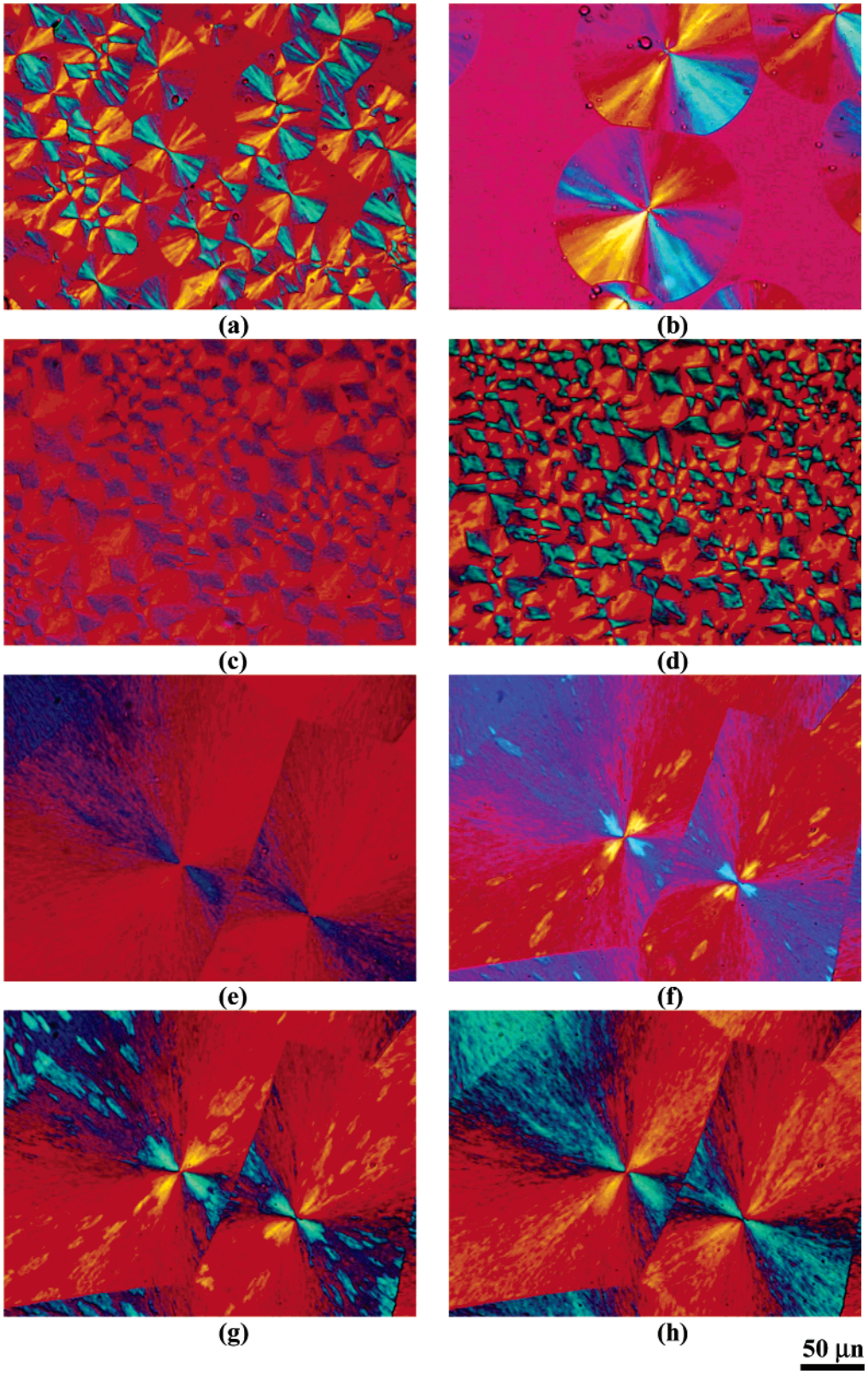

Figure 16. Polarized optical micrographs during isothermal crystallization: (a) homo-PLLA, after 4 min at 100 °C; (b) homo-PLLA, after 6 min at 120 °C; (c) $L_{44}{}^{11}C_{56}{}^{14}$ after 30 min at 100 °C; (d) same sample as (c), 6 min after the temperature was lowered and equilibrated at 30 °C; (e) $L_{44}{}^{11}C_{56}{}^{14}$ after 30 min at 120 °C. The temperature was lowered to 30 °C after picture (e) was taken, and then the following images were captured: (f) $L_{44}{}^{11}C_{56}{}^{14}$ after 20 s at 30 °C; (g) $L_{44}{}^{11}C_{56}{}^{14}$ after 40 s at 30 °C; (h) $L_{44}{}^{11}C_{56}{}^{14}$ after 5 min at 30 °C.

can be seen to spread through the spherulite in Figure 16g to yield a final homogeneous spherulitic texture in Figure 16h, where quadrants 1 and 3 have a color that is more yellow in tone and 3 and 4 are lighter blue. The diblock copolymer spherulites are very similar to homo-PLLA spherulites. The resulting morphology is that of mixed spherulites where crystalline PLLA and PCL lamellae are probably separated by mixed PLLA/PCL amorphous interlamellar regions. The sherulitic morphology of $L_{60}{}^{12}C_{40}{}^{9}$ was also very similar to homo-PLLA

(results not shown). It is worth noting that a morphology of interdigitized lamellae has been obtained before for weakly segregated and also double crystalline poly(*p*-dioxanone)-*b*-poly(ϵ-caprolactone) diblock copolymers.[6−8]

Conclusions

The PLLA-*b*-PCL diblock copolymers studied in this work were miscible in the melt according to both SAXS and DSC evidence. However, upon cooling from the melt at 165 °C, the sample $L_{60}{}^{12}C_{40}{}^{9}$ transformed into a transient microphase-separated lamellar structure in the melt at 100 °C just before crystallization started, a fact that needs further study.

When the diblock copolymers were crystallized isothermally at 100 °C, only the PLLA block was able to crystallize. Crystallization drove structure formation, and PLLA spherulites were formed. The crystallization kinetics of the PLLA block was determined by both DSC and time-resolved WAXS. An Avrami analysis of the data indicated that three-dimensional superstructures were formed from instantaneous nuclei ($n = 3$). This was confirmed by the observation of spherulites in POM. The crystallization kinetics was not so different from homo-PLLA and was weakly dependent on composition in the narrow range examined here.

The PCL block behaved very differently when it was subsequently crystallized by quenching the samples to 30 °C (after PLLA crystallization). It crystallized within the PLLA previously formed spherulites as intraspherulitic lamellae; the resulting mixed spherulites were very similar to homo-PLLA negative spherulites except for subtle birefringence changes. An Avrami analysis of DSC data yielded a result compatible with these POM observations, i.e., two-dimensional structures formed by instantaneous nucleation ($n = 2$). The PCL block crystallization in $L_{44}{}^{11}C_{56}{}^{14}$ was 4 times slower than homo-PCL, and in the case of $L_{60}{}^{12}C_{40}{}^{9}$ the difference was much bigger (21 times slower than homo-PCL). Such a highly dependent value on composition is related to topological restrictions caused by the previous crystallization of the covalently linked PLLA block.

Acknowledgment. This work was supported by EPSRC Grant GR/S73037/01. X-ray data peak fitting program xfit is provided by CCP13, the collaborative project for fiber diffraction data analysis. We are grateful to Dr. Sasha Mykhaylyk (University of Leeds) for assistance in calculating WAXS patterns for PCL and PLLA. The USB team acknowledges sponsorship by Fonacit (Grant S1-2001000742). SMPC is much indebted to the Région Wallonne and the Fonds Social Européen for support in the frame of Objectif 1-Hainaut: Materia Nova as well to the Belgian Federal Government Office of Science Policy (PAI 5/3).

References and Notes

(1) Hamley, I. W. *The Physics of Block Copolymers*; Oxford University Press: Oxford, 1998.
(2) Hamley, I. W. *Adv. Polym. Sci.* **1999**, *148*, 113.
(3) Loo, Y. L.; Register, R. A. Crystallization within block copolymer mesophases. In Hamley, I. W., Ed.; *Developments in Block Copolymer Science and Technology;* Wiley: New York, 2004; p 213.
(4) Müller, A. J.; Balsamo, V.; Arnal, M. L., *Adv. Polym. Sci*., in press.
(5) Bezwada, R. S.; Jamiolkowski, D.; Cooper, K. In *Handbook of Biodegradable Polymers*; Domb, A. J., Kost, J., Wiseman, D. M., Eds.; Harwood: Singapore, 1997; Chapter 2, pp 29−61.
(6) Albuerne, J.; Márquez, L.; Raquez, J. M.; Degée, Ph.; Dubois, Ph.; Castelletto, V.; Hamley, I. W. *Macromolecules* **2003**, *36*, 1633.
(7) Müller, A. J.; Albuerne, J.; Esteves, L. M.; Márquez, L.; Raquez, J. M.; Degée, Ph.; Dubois, Ph.; Collins, S.; Hamley, I. W. *Macromol. Symp.* **2004**, *215*, 369.
(8) Müller, A. J.; Albuerne, J.; Marquez, L.; Raquez, J. M.; Degée, Ph.; Dubois, Ph.; Hobbs, J.; Hamley, I. W. *Faraday Discuss.* **2005**, *128*, 231.
(9) Bogdanov, B.; Vidts, A. E.; Berghmans, H. *Macromolecules* **1999**, *32*, 726.
(10) Kim, J. K.; Park, D. J.; Lee, M. S.; Ihn, K. J. *Polymer* **2001**, *42*, 7429.
(11) Ho, R. M.; Hsieh, P. Y.; Tseng, W. H.; Lin, C. C.; Huang, B. H.; Lotz, B. *Macromolecules* **2003**, *36*, 9085.
(12) Bhattarai, N.; Kim, H. Y.; Cha, D. I.; Lee, D. R.; Yoo, D. I. *Eur. Polym. J.* **2003**, *39*, 1365.
(13) Kim, K.-S.; Chung, S.; Chin, I.-J.; Kim, M.-N.; Yoon, J.-S. *J. Appl. Polym. Sci.* **1991**, *72*, 341.
(14) Dubois, Ph.; Jacobs, C.; Jerome, R.; Teyssie, Ph. *Macromolecules* **1991**, *24*, 3027.
(15) Tang, C. C.; Martin, C. M.; Laundy, D.; Diakun, G. P. *Nucl. Instrum. Methods Phys. Res., Sect. B*, in press. Helsby, W. I.; Berry, A.; Buksh, P. A.; Hall, C. J.; Lewis, R. A. *Nucl. Instrum. Meth. A* **2003**, *510*, 138.
(16) Cernik, R. J.; Barmes, P.; Bushnell-Wye, G.; Dent, A. J.; Diakun, G. P.; Flaherty, J. V.; Greaves, G. N.; Heeley, E. L.; Helsby, W.; Jacques, S. D. M.; Kay, J.; Rayment, T.; Ryan, A. J.; Tang, C. C.; Terrill, N. J. *J. Synchrotron Rad.* **2004**, *11*, 163.
(17) Gedde, U. W. *Polymer Physics*; Chapman and Hall: London, 1995.
(18) Sasaki, S.; Asakura, T. *Macromolecules* **2003**, *36*, 8385.
(19) Chatani, Y.; Okita, Y.; Tadokoro, H.; Yamashita, Y. *Polym. J.* **1970**, *1*, 555.
(20) Hamley, I. W.; Castelletto, V. *Prog. Polym. Sci.* **2004**, *29*, 909.
(21) Leibler, L. *Macromolecules* **1980**, *13*, 1602.
(22) de Gennes, P. G. *J. Phys. (Paris)* **1970**, *31*, 235.
(23) Stoiber, E.; Morse, S. A. *Crystal Identification with the Polarizing Microscope*; Chapman and Hall: New York, 1994.

MA0481499